INVESTIGATION OF OSCILLATIONS OF THE COEFFICIENT OF ABSORPTION OF SOUND IN ANTIMONY

A. P. KOROLYUK and L. Ya. MATSAKOV

Institute of Radiophysics and Electronics, Academy of Sciences, Ukrainian S.S.R.

Submitted to JETP editor September 7, 1966

J. Exptl. Theoret. Phys. (U.S.S.R.) 52, 415–423 (February, 1967)

The oscillations of the coefficient of ultrasound absorption in single-crystal antimony were investigated at helium temperatures and at longitudinal-oscillation frequencies 500 MHz in three principal crystallographic planes. The extremal momenta of the Fermi surface were determined. The experimental data were used to construct the projections of the electronic and hole surfaces on the plane of the trigonal and bisector axes. The deviation of the equal-energy surfaces of antimony from ellipsoids is discussed. The results are compared with data on the de Haas–van Alphen effect in antimony.

INTRODUCTION

THE electronic properties of the elements of the fifth group of the periodic system—bismuth, antimony, and arsenic—were subjected for many years to an intense study both from the theoretical and experimental points of view. The main features of the spectrum of these substances can be understood by recognizing that their unit cell consists of two ions with five valence electrons each. These ten electrons in the cell fill completely the five energy bands, and if the crystal lattice were cubic, all these elements would be dielectrics.[1] Since actually the lattice is rhombohedral (slightly deformed cube), the fifth and sixth bands overlap, as a result of which an equal number of electrons and holes appear in the conduction and valence bands. These carriers form small surfaces in the Brillouin zone, and the form of the surfaces is close to ellipsoidal, making it possible to approximate, with good accuracy, the electronic properties with the aid of a small number of parameters.

A study of the de Haas–van Alphen effect,[2-6] the Shubnikov–de Haas effect,[7-9] cyclotron resonance,[10] ultrasound absorption,[11-13] and infrared absorption[14] has confirmed experimentally the foregoing concepts. For antimony, for example, it was found that the Fermi surfaces are nearly ellipsoidal in form.

Certain confusion existed for a long time with respect to the number of ellipsoids and their exact placement and dimensions. It was impossible to attain the compensation of the volumes of the electron and hole surfaces, which is necessary to explain the semimetallic properties of antimony. In recent papers,[4,5] using a new spectroscopic procedure for the investigation of the de Haas–van Alphen effect, it was shown that the hole ellipsoids are stretched along one of the axes, which is inclined to the base plane of the crystal by an angle of approximately 34°, and the long axis of the electronic ellipsoids is inclined at ~4° to the same plane. Compensation of the volume takes place if it is assumed that there are two hole ellipsoids for each electron ellipsoid.

The first investigations of geometric resonance in antimony were carried out by Eckstein[11] and by Eriksson, Beckman, and Hornfeldt.[13] Their results are preliminary in character. It seemed of interest, using an improved procedure and higher ultrasonic frequencies, to attempt to obtain detailed information on the extremal dimensions and form of the Fermi surface of antimony.

We measured the anisotropy of the periods of the oscillations of geometrical resonance in the three principal crystallographic planes of single-crystal antimony at longitudinal sound frequencies of 500 MHz in a magnetic field up to 3000 Oe at temperatures 1.4–4.2° K.

MEASUREMENT PROCEDURE

The periods of the oscillations of the absorption coefficient of the ultrasound when measured with an ultrasonic spectrometer operating in the continuous mode. Its block diagram is described in [15]. The electromagnetic energy was converted into sound by quartz X-cut plates whose natural

resonant frequency was approximately 100 MHz. The plates were excited at harmonics of the resonant frequency.

The samples, in forms of discs 8 mm in diameter were cut with an electric-spark lathe with accuracy not worse than 1° out of single-crystal antimony of Su-000 grade, subjected to twenty zone recrystallizations. The sample thickness was ~2.5 mm. By subsequent polishing with fine abrasive, the ends were made sufficiently plane-parallel for ultrasonic measurements.

The mounting of the samples relative to the magnetic field, in the planes of the binary and of the binary and trigonal axes, was in accord with the magnetic-symmetry pictures. The following procedure was used in the asymmetrical plane of the bisector and trigonal axes. The sample was cleaved along the basal plane. The base of a cylindrical test coil, wound of thin copper wire, was clamped against the cleavage plane in such a way that the plane of the winding turns was parallel to the plane of the base. The instrument with the sample was mounted in the field of an electromagnet, whose coil carried small alternating current. The minimum voltage on the test coil, observed as the electromagnet was rotated, corresponded to the orientation of the trigonal axis perpendicular to the magnetic force lines.

The accuracy of orientation of the samples by such a method was determined by the accuracy with which the coil was manufactured and by the quality of the cleaved plane. In our case the error of mounting the sample relative to the direction of the field did not exceed ±0.5°.

The oscillograms, as functions of the reciprocal magnetic field, constitute superpositions of several sinusoidal components with different amplitudes, which depend on the field intensity. The analysis problem consists of separating and measuring the period of each component. In the case of two-component curves with slightly differing periods or three-component curves with strongly different period of one of the components, the analysis usually entails no great difficulty. Actually, it is more frequently necessary to analyze curves having an arbitrary ratio of the amplitudes and periods of the oscillating components.

Two methods were used to "improve" the ratio of the amplitudes in a complicated curve and to facilitate the analysis: recording the derivatives of higher order, and modulation of the magnetic field at an angle to the main field. It can be shown that for an oscillating curve consisting of a superposition of two sinusoidal components, the ratio of the amplitudes A_2/A_1 ($A_1 > A_2$) increases by a factor $(T_1/T_2)^n$ when the n-th derivative is recorded (T_1 and T_2 are the periods of the first and second components).

As shown in [5, 16], by choosing the angle between the direction of the constant magnetic field and the vector of the modulating field it is possible to attenuate greatly, and sometimes even suppress completely the components of the oscillations. To this end we used two pairs of modulating coils, placed perpendicular to each other in the gap of the electromagnet. The direction of the vector of the modulating field was determined by the ratio of the currents and phases in these coils, and could be oriented at an arbitrary angle to the direction of the constant magnetic field.

The use of modulation at an angle and of recording the high-order derivatives made it possible to determine the periods of the oscillations in many important crystallographic directions.

The magnetic field vector **H** was perpendicular to the sound wave vector **k** in all the experiments.

EXPERIMENTAL RESULTS

Recent theoretical calculations of the Fermi surface of antimony[17] show that it consists of three equivalent electronic surfaces, representing ellipsoids which are slightly deformed in their central parts, and six hole surfaces, which differ greatly from ellipsoids. For an experimental study of the shape and dimensions of the Fermi surface of antimony, we measured the periods of the oscillations of the geometric resonance.

As is well known,[18] the extremal diameter of the external Fermi surface D_{ext} in the $\mathbf{k}\times\mathbf{H}$ direction is connected with the period of the oscillations of the geometrical resonance ΔH^{-1} by the relation

$$D_{ext} = e\lambda / c\Delta H^{-1}, \qquad (1)$$

where e is the electron charge, c the velocity of light, and $\lambda = 2\pi/k$ is the wavelength of sound.

The periods of the oscillations were measured experimentally at three orientations of the crystal axes relative to the wave vector **k** of the sound: a) **k** parallel to the binary axis, **H** rotating in the plane of the trigonal and binary axes; b) **k** parallel to the bisector axis, **H** rotating in the plane of the trigonal and binary axes; c) **k** parallel to the trigonal axis, **H** rotating in the plane of the binary axes.

Figure 1 shows a sample plot of the derivative of the absorption coefficient $d\Gamma/dH$ against the reciprocal magnetic field for a wave vector **k** parallel to the binary axis, and for **H** oriented in

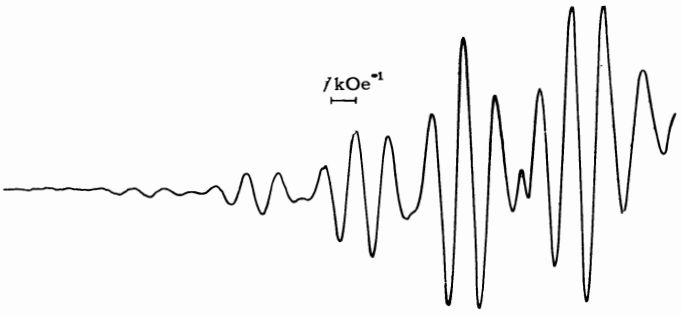

FIG. 1. Plot of the derivative $d\Gamma/dH$ of the absorption coefficient of sound vs. the reciprocal of the magnetic field 1/H. The wave vector of sound **k** is directed along the binary axis, and **H** makes an angle 97° to the trigonal axis, $\mathbf{k} \perp \mathbf{H}$.

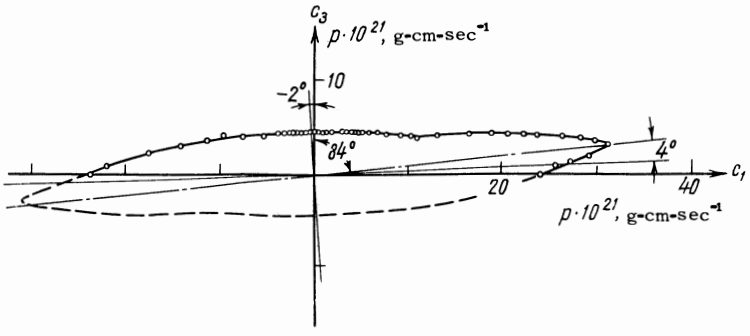

FIG. 2. Projection of the electronic surface on the plane of the trigonal and bisector axes. The letters c_1 and c_3 denote respectively the bisector and trigonal axes.

the plane of the trigonal and bisector axes at an angle 97° to the trigonal axis.

The experimental results obtained for orientation a) are shown in Figs. 2 and 3. Figure 2 shows the anisotropy of the extremal diameters of the Fermi surface in a polar coordinate system for the electrons. A similar dependence for holes is shown in Fig. 3. The extremal diameters of the Fermi surface in momentum space were determined from the measured periods of the geometric-resonance oscillations with the aid of formula (1).

It must be noted that the hole component of the oscillations in the case of orientation a) is strongly masked by the electronic component, especially in the region of angles adjacent to the directions of the maximum diameters. Only by using the procedure described above were we able to trace the hole component of the oscillations in the entire region of investigated angles.

Figure 4 shows results obtained for orientation b). The oscillation periods with maximum at 90° are connected with the electronic surface, the remaining periods are connected with the hole surface. The oscillations are much weaker in this case than for orientation a), and only in the angle region from 60 to 120° does the electronic component become quite intense. Compared with [11], we observed oscillations of the hole surface in this plane, and also were able to trace the electronic

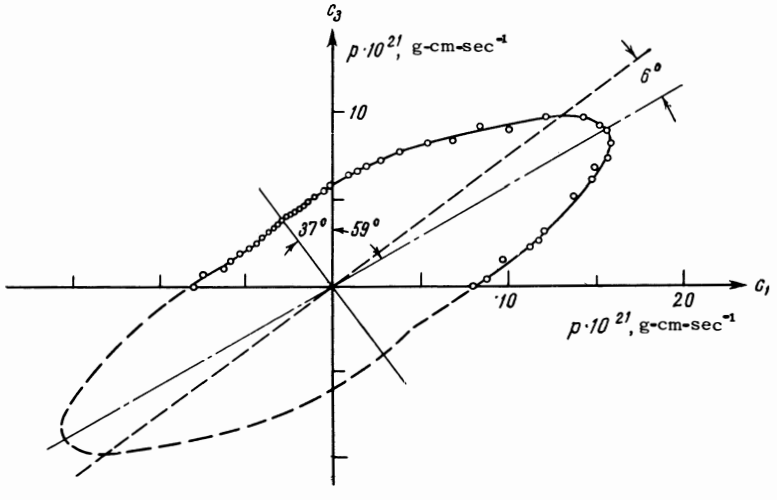

FIG. 3. Projection of the hole surface on the plane of the trigonal (c_3) and bisector (c_1) axes.

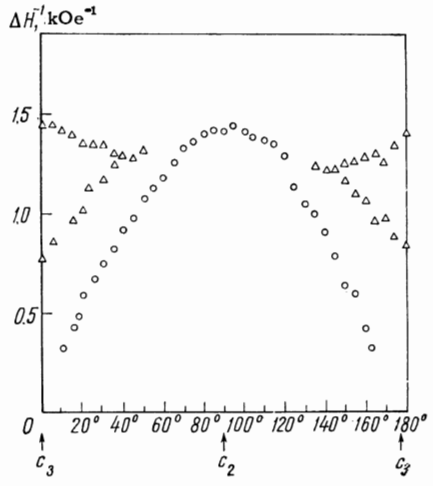

FIG. 4. Geometric-resonance oscillation periods vs. direction of the magnetic field. ○–electron periods, △–hole periods. The sound wave vector **k** is parallel to the bisector axes, **H** lies in the plane of the trigonal (c_3) and binary (c_2) axes.

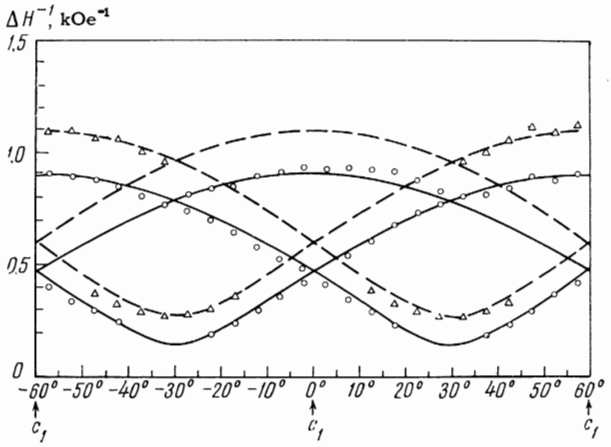

FIG. 5. Dependence of the periods of the oscillations of the geometrical resonance on the direction of the magnetic field: ○–electron periods, △–hole periods. The sound wave vector **k** is parallel to the trigonal axis, and **H** lies in the plane of the binary axes.

oscillations in a much larger angle interval. This plane was not investigated by the authors of [13].

The experimental results obtained for orientation c) are shown in Fig. 5. The same figure shows the theoretically calculated (in a quadratic approximation) course of the anisotropy of the periods for the electrons (solid lines) and for holes (dashed lines). The intense oscillations are those of the electronic surface, to which the lower curves correspond in the figure. In the angle region from $-40°$ to $-20°$ and from $+20$ to $+40°$, these oscillations vanish and the remaining components are connected with hole surface. In this plane we observed for the first time the oscillation periods of the geometric resonance of the hole surface, making it possible to determine its extremal diameter in the direction of the binary axis.

We present below results of our measurements of the main Fermi-surfaces parameters which do not depend on the models of the electronic spectrum.

1. The minimum momentum values are $p_1^e = (4.63 \pm 0.14) \times 10^{-21}$ for the electrons[1)] and $p_1^h = (3.92 \pm 0.12) \times 10^{-21}$ for the holes. The directions of p_1^e and p_1^h coincide with those of the binary axis.

2. The maximum momentum is $p_2^e = (31.4 \pm 0.9) \times 10^{-21}$ for the electrons and $p_2^h = (18.0 \pm 0.5) \times 10^{-21}$ for the holes. The direction in which p_2^e reaches a maximum is inclined 84° to the trigonal axis in the plane of the trigonal and bisector axes. For p_2^h this angle amounts to 59°.

3. The minimum momentum in the plane of the bisector and trigonal axes is $p_3^e = (4.50 \pm 0.14) \times 10^{-21}$ for the electrons and $p_3^h = (4.79 \pm 0.15) \times 10^{-21}$ for the holes. The value of p_3^e reaches a minimum in a direction inclined $-2°$ to the trigonal axis; for holes this angle is $-37°$.

It is of interest to compare the experimental data concerning the directions of the extremal values of the section areas of the surfaces, obtained by Windmiller[5] and by Brandt et al.,[6] and the directions of the magnetic field for the extremal momenta, determined in the present paper, with the theoretical calculations of Falicov and Lin.[17] These results are summarized for the plane of the trigonal and bisector axes in Table I (the angle is reckoned from the trigonal axis). It is seen from the table that certain experimental and theoretically-calculated inclination angles for electrons are in good agreement. For holes the angles of inclination of the minimal section of the surface is calculated approximately and the disparity with experiment is more noticeable.

DISCUSSION OF RESULTS

For convenience in the subsequent exposition we introduce a system of axes p_1, p_2, p_3 connected with the centers of the ellipsoids, directing p_1 along the binary axis of the crystal, p_2 along the direction of maximum elongation, and p_3 in a direction perpendicular to p_1 and p_2. The principal sections of the ellipsoids $p_1 = 0$, $p_2 = 0$, and $p_3 = 0$ are denoted respectively by S_1, S_2, and S_3.

The projections of the extremal diameters on the plane of the trigonal and bisector axes, shown

1)All the values of the momenta presented here and below have dimension g-cm-sec^{-1}.

Table I

Type of carrier		Angle between trigonal axis and the direction to the extremal period of the de Haas–van Alphen oscillations and the oscillations of geometrical resonance			
		Theory [17]	Experiment [5]	Experiment [4]	Experiment Present work
Electrons	Maximum period	87.5°	87,7°	87.6°	88.0°
	Minimum period	173°	174°	175.5°	174°
Holes	Maximum period	41°	53°	53°	53°
	Minimum period	—	148.8°	149°	149°

in Figs. 2 and 3, could be constructed because of the presence of an accurately measured dependence of the oscillation periods on the direction of the magnetic field in the entire interval of the investigated angles. It must be emphasized that the construction figures are correct (correspond to the true projections of the Fermi surface) only if the sections of the surface are convex and centrally symmetrical in the given crystallographic plane. The symmetry center exists, at any rate, in the electronic surfaces,[17] so that out of the two projections shown in Figs. 2 and 3, the one that is correct with the greater probability is that shown in Fig. 2.

It is clearly seen from Figs. 2 and 3 that the projections of the extremal diameters on the plane of the trigonal and bisector axes differ from the ellipses that should be observed in the case of a quadratic energy dispersion law. In the plane of the binary axes, the anisotropy of the periods of the geometric-resonance oscillations coincides practically with those calculated by the quadratic model (Fig. 5).

Table II lists data illustrating the quantitative deviations of the form of the surfaces from ellipsoids (for convenience in comparison with [5, 6], the values of the areas are given in atomic units, i.e., it is assumed that $e = m = \hbar = 1$, the unit length is the Bohr radius $a_0 = 0.529$ Å). The areas of the extremal cross sections, measured with the aid of the de Haas–van Alphen effect, are compared with the areas of the ellipses constructed with the corresponding momenta taken as the ellipse semiaxis, as calculated from our data.

The asterisk in Table II denotes results of area measurements obtained by numerical integration by means of the formula

$$S = \frac{1}{2}\int p^2\, d\varphi \qquad (2)$$

for the p_2p_3 plane. The area obtained in this manner for electrons is 11% smaller than that calculated by the ellipsoidal model and agrees better with that measured by the de Haas–van Alphen effect. It can be therefore concluded that the obtained form of the projections (Fig. 2) of the extremal diameters on the p_2p_3 plane is apparently close to the form of the central section $p_1 = 0$ for the electrons.

For holes the result of the numerical integration coincides in practice with the calculation for the ellipsoidal model (difference 1.5%), although the form of the projection is clearly not ellipsoidal. In addition, it is seen that the area of the

Table II

$S_1 \cdot 10^5$	$S_2 \cdot 10^3$	$S_3 \cdot 10^3$	$n \cdot 10^{-19}$	Data of
		Electrons		
11.2 ±0.7	1,65±0,16	11.5±0.7	5.65±0,51	The authors'
9.98±0.60*				
9.61	1.82	11.6	5.54	[5]
9.62	1.82	11.5	5.36	[6]
		Holes		
6.82±0.41	1,48±0,16	5.58±0.35	5.82±0,52	The authors'
6.90±0.41*				
5.77	1.637	5.28	5,49	[5]
5.7	1,61	5.19	5.36	[6]

*Obtained by numerical integration (the remaining quantities were calculated using the ellipsoidal model).

projection is 20% larger than the area of the corresponding extremal section of the hole surface S_1. Apparently, the obtained projection on the p_2p_3 plane for holes does not correspond to the form of the central section of the hole surface.

The remaining values of the parameters of the surfaces, as well as the densities of the electrons and the holes, calculated on the basis of our measurements, agree within the limits of errors with the corresponding quantities obtained from results on the oscillations of the magnetic susceptibility. It is interesting to note that all the singular directions on the angle diagrams for the de Haas–van Alphen effect and the geometric oscillations (Table I) coincide within the limits of errors. For convex surfaces, such a situation is perfectly obvious, but for a surface of arbitrary form the coincidence of the directions to the extrema of the momenta and the cross section areas is not obligatory. At any rate, in calculating the electronic spectrum of antimony it is necessary to take this circumstance into account.

Judging from the deviation of the form of the sections from ellipsoidal, we can also expect the energy dispersion to deviate from quadratic and, as correctly noted in [6], such deviations can be quite appreciable. In the case of quadratic energy dispersion, the effective masses should be inversely proportional to the corresponding electron momenta. The comparison made by us has shown that the mass ratio by Datars and Vanderkooy[10] is not always inversely proportional to the corresponding momenta. The greatest deviations (up to 90%) are observed for electrons with relatively large momenta (p_2). For small momenta and masses the deviations from quadratic are smaller. Starting from this comparison we can conclude that the quadratic approximation in the expansion of the energy by momenta near the points of minima and maxima can be used for momentum values $p \leq (5 - 7) \times 10^{-21}$.

In conclusion we present the parameters of the spectrum of antimony in the quadratic approximation (Table III) obtained from our experiments:

Quantity:	m_{11}	m_{22}	m_{33}	m_{23}	E_F, erg
Electrons:	0.112	4.19	0.107	1.55	$10.5 \cdot 10^{-14}$
Holes:	0.057	0.237	0.121	0.199	$14.7 \cdot 10^{-14}$

The values of the cyclotron masses used to determine E_F were taken from [10]. The data can be used if account is taken of their approximate character and the foregoing remark.

[1] A. A. Abrikosov and L. A. Fal'kovskiĭ, JETP **43**, 1089 (1962), Soviet Phys. JETP **16**, 769 (1963).

[2] D. Shoenberg, Phil. Trans. Roy. Soc. London, **A245**, 1 (1952).

[3] Y. Saito, J. Phys. Soc. Japan **18**, 425 (1963).

[4] L. R. Windmiller and M. G. Priestly, Solid State Commun. **3**, 199 (1965).

[5] L. R. Windmiller, Phys. Rev. (in press).

[6] N. B. Brandt, N. Ya. Minina, and Chu Chenkang, JETP **51**, 108 (1966), Soviet Phys. JETP **24**, 73 (1967).

[7] J. Ketterson and Y. Eckstein, Phys. Rev. **132**, 1885 (1963).

[8] L. S. Lerner and P. C. Eastman, Can. J. Phys. **41**, 1523 (1963).

[9] G. N. Rao, N. H. Zebouni, C. G. Grenier, and J. M. Reynolds, Phys. Rev. **133**, A141 (1964).

[10] W. R. Datars and J. Vanderkooy, IBM J. Res. Develop. **8**, 247 (1964).

[11] Y. Eckstein, Phys. Rev. **129**, 12 (1963).

[12] J. B. Ketterson, Phys. Rev. **129**, 18 (1963).

[13] L. Eriksson, O. Beckman, and S. Hornfeldt, J. Phys. Chem. Sol. **25**, 1339 (1964).

[14] C. Nannely, Phys. Rev. **129**, 109 (1963).

[15] A. P. Korolyuk, JETP **49**, 1009 (1965), Soviet Phys. JETP **22**, 701 (1966).

[16] V. S. Édel'man, E. P. Vol'skiĭ, and M. S. Khaĭkin, PTÉ No. 3, 179 (1966).

[17] L. M. Falicov and P. J. Lin, Phys. Rev. **141**, 562 (1966).

[18] V. L. Gurevich, JETP **37**, 71 (1959), Soviet Phys. JETP **10**, 51 (1960).

Translated by J. G. Adashko
53